Geomechanics and Engineering, *Vol. 26, No. 1 (2021) 41-47*
https://doi.org/10.12989/gae.2021.26.1.041

Hoek-Brown failure criterion for damage analysis of tunnels subjected to blast load

Farhad Chinaei[1], Kaveh Ahangari*[1] and Reza Shirinabadi[2]

[1]*Department of Mining Engineering, Science and Research Branch, Islamic Azad University, Tehran, Iran*
[2]*Department of Petroleum and Mining Engineering, South Tehran Branch, Islamic Azad University, Tehran, Iran*

(Received March 29, 2021, Revised June 12, 2021, Accepted June 24, 2021)

Abstract. In this study, a rock tunnel subjected to blast load is modeled mathematically. For this purpose, a cylindrical shell element is used and the motion equations are derived by energy method and Hamilton's principle. In the inner surface of tunnel, different blast holes are considered and its force in radial direction is coupled by motion equations. The structural damping of the structure is assumed by Kelvin-Voigt model. Hoek-Brown failure criterion is utilized for explosion damage analysis of the tunnel. The motion equations are solved numerically by differential quadrature method (DQM). The effect of different parameters such as depth of tunnel, number and diameter of blast holes, type of stone, geological strength index (GSI) and density of stone, type and mass of explosive material are studied on the damage factor of Hoek-Brown criterion. Numerical results show that with increasing the density of explosive material, number and diameter of blast holes, the thickness of damage is increased in the tunnel. In addition, the depth of damage is decreased with increasing strength, GSI, density of rock and depth of tunnel.

Keywords: blasting; GSI; Hoek-Brown failure criterion tunnel; mathematical modelling; numerical method

1. Introduction

The failure criterion of Hoek-Brown and the related GSI are achieved good admission for calculating the deformation and strength characteristics of rock masses. Due to the lack of appropriate alternatives, this criterion is accepted by the community of rock mechanics and its application rapidly deployed beyond the original consideration based on admixing joint-defined blocks in the hard rocks.

In the field of mathematical modelling of structures, Kumar *et al.* (2013) investigated vibration of cylindrical sandwich shells utilizing Zigzag theory. Duc and Then (2015) presented vibrations and dynamic analysis of functionally graded cylindrical shells. Seo *et al.* (2015) studied vibration response of cylindrical shells with internal fluid utilizing finite element solution prosidure. A combined numerical methods based on finite element was applied by Nguyen-Hoang *et al.* (2016) for dynamic analysis of Reissner–Mindlin shells. Katariya and Panda (2019) studied frequency, deflection and transient responses of the sandwich layered shell structure subjected to different mechanical loading. The flexural free vibration of honeycomb thin-walled cylindrical sandwich shell was studied by Li *et al.* (2020) based on Flügge's shell theory and experiments. Zhang *et al.* (2020a) presented dynamic and static responses of cylindrical shell utilizing finite elements method. Keshtegar *et al.* (2020) studied dynamic stability response of a sandwich nanocomposite truncated conical shells utilizing differential cubature method. Vibration response of a circular thin cylindrical shell based on finite element method was presented byRawat *et al.* (2020). Tran *et al.* (2020) studied the numerical free-vibration response of a functionally graded stiffened cylindrical shell embedded in Winkler–Pasternak foundation.

Tunnels dynamic analysis was studied by some reserchers. Recently, Rashiddel *et al.* (2020) investigated a tunnel lining and its segmentation with curved and planar joints subjected to dynamic loads. Zhang *et al.* (2020b) applied a numerical method for dynamic analysis of methane-hydrogen explosion in utility tunnels. Numerical analysis for damage probability in the mine tunnel subjected to explosion of a hydrogen-air mixture was presented by Skob *et al.* (2020). Hajihassani *et al.* (2020) studied 3D prediction of tunnel subjected to ground movements. Tiwari *et al.* (2020) presented 3D nonlinear finite element response in curved under the internal blast loading. Effects of liner geofoam on circular tunnels resting on soil medium under the blast loading were studied by Han *et al.* (2020). Zhao *et al.* (2020) applied a 3D modelling for investigating the dynamic of tunnels under the blast load. Zaid and Rehan Sadique (2020) investigated dynamic analysis of rock tunnel subjected to blast load utilizing finite element method. Iwano *et al.* (2020) focused on the reduction of tunnel blasting utilizing advanced electronic detonators. Molkov and Dery (2020) studied blast wave decay correlation obtained for hydrogen tank in a tunnel fire. Wu *et al.* (2020) studied mechanical response of circular Tunnels with double primary linings in squeezing grounds. A three-dimensional (3D) finite element program was used

*Corresponding author, Professor
E-mail: kaveh.ahangari@gmail.com

ISSN: 2005-307X (Print), 2092-6219 (Online)

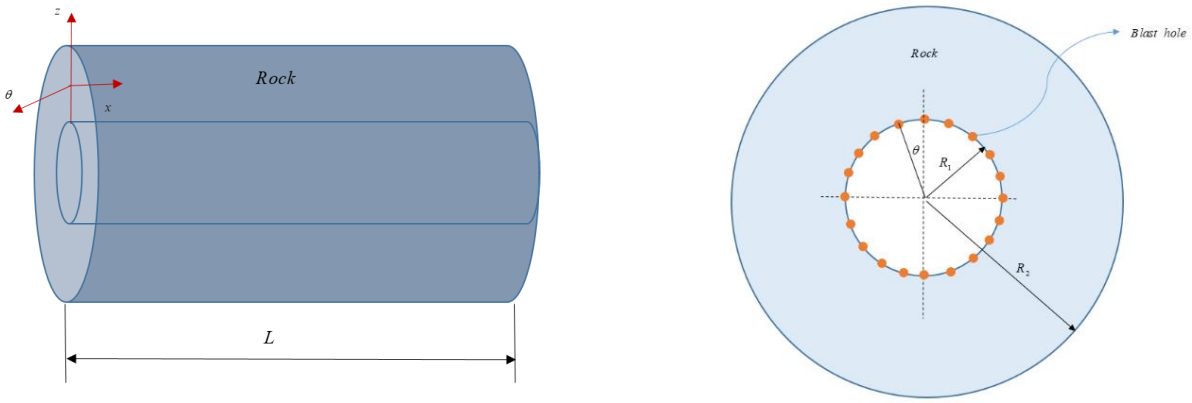

Fig. 1 Scheme of tunnel with different blast holes

by Chen and Li (2020) for the analysis of various horseshoe-shaped opening expressway tunnels under different geologies. The interactive effects between existing structures and surrounding ground due to the excavation of the divergence tunnel was studied by Hong *et al.* (2020). Experimental study on the mechanical response and failure behavior of double-arch Tunnels with cavities behind the liner was investigated by Zhang *et al.* (2020).

So far, no studies have been done about mathematical modelling and numerical damage analysis of tunnels under the blast load. Hence, a viscoelastic rock tunnel subjected to blast load is modeled mathematically based on cylindrical shell theory. In the inner surface of tunnel, different blast holes are considered and its force in radial direction is coupled by motion equations. Hoek-Brown failure criterion and DQM are utilized for explosion damage analysis of the tunnel. The effect of different parameters such as depth of tunnel, number and diameter of blast holes, type of stone, geological strength index (GSI) and density of stone, type and mass of explosive material are studied on the failure factor of Hoek-Brown criterion.

2. Mathematical modeling

Fig. 1 shows a tunnel modeled by a circular cylindrical shell with the inner radius of R_1, outer radius of R_2 and length of L and the cylindrical coordinate system of (x, θ, z). At the inner surface of tunnel, different blast holes are assumed.

In this paper, classical theory is used. Displacement field can be expressed as below based on the classic theory (Reddy 2004):

$$u_1(x,\theta,z,t)=u(x,\theta,t)-z\frac{\partial w(x,\theta,t)}{\partial x}, \tag{1}$$

$$u_2(x,\theta,z,t)=v(x,\theta,t)-\frac{z}{R}\frac{\partial w(x,\theta,t)}{\partial \theta}, \tag{2}$$

$$u_3(x,\theta,z,t)=w(x,\theta,t), \tag{3}$$

in which (u,v,w) are the displacement of the middle plane (z=0) in the (x,θ,z) directions, respectively. The relationships of strain-displacement are

$$\varepsilon_{xx}=\frac{\partial u}{\partial x}-z\frac{\partial^2 w}{\partial x^2}, \tag{4}$$

$$\varepsilon_{\theta\theta}=\frac{\partial v}{R\partial\theta}+\frac{w}{R}-\frac{z}{R^2}\frac{\partial^2 w}{\partial\theta^2}, \tag{5}$$

$$\varepsilon_{xy}=\frac{1}{2}\left(\frac{\partial u}{R\partial\theta}+\frac{\partial v}{\partial x}\right)-z\frac{\partial^2 w}{R\partial x\partial\theta}, \tag{6}$$

The strain-stress relationships are simplified as (Reddy 2004):

$$\begin{bmatrix}\sigma_{xx}\\ \sigma_{\theta\theta}\\ \tau_{x\theta}\end{bmatrix}=\begin{bmatrix}C_{11} & C_{12} & 0\\ C_{21} & C_{22} & 0\\ 0 & 0 & C_{66}\end{bmatrix}\begin{bmatrix}\varepsilon_{xx}\\ \varepsilon_{\theta\theta}\\ \gamma_{x\theta}\end{bmatrix}, \tag{7}$$

The potential energy of the structure is as the following:

$$U=\int_V\left(\sigma_{xx}\varepsilon_{xx}+\sigma_{\theta\theta}\varepsilon_{\theta\theta}+\sigma_{x\theta}\gamma_{x\theta}\right)dV, \tag{8}$$

By replacing the strain equations in the above relationships, we have

$$U=\int_{-\frac{h}{2}}^{\frac{h}{2}}\iint_A\left(\sigma_x\left(\frac{\partial u}{\partial x}+0.5\left(\frac{\partial w}{\partial x}\right)^2-z\frac{\partial^2 w}{\partial x^2}\right)+\sigma_\theta\left(\frac{\partial v}{R\partial\theta}+\frac{w}{R}+0.5\left(\frac{\partial w}{R\partial\theta}\right)^2\right.\right.$$
$$\left.\left.-z\frac{\partial^2 w}{R^2\partial\theta^2}\right)+\sigma_{x\theta}\left(\frac{\partial u}{R\partial\theta}+\frac{\partial v}{\partial x}+\frac{\partial w}{R\partial\theta}\frac{\partial w}{\partial x}-2z\frac{\partial^2 w}{R\partial\theta\partial x}\right)\right)dz\,dA \tag{9}$$

By defining the energy and intra –plane moments as below,

$$\begin{Bmatrix}N_x\\ N_\theta\\ N_{x\theta}\end{Bmatrix}=\int_{-\frac{h}{2}}^{\frac{h}{2}}\begin{Bmatrix}\sigma_x\\ \sigma_\theta\\ \tau_{x\theta}\end{Bmatrix}dz, \tag{10}$$

$$\begin{Bmatrix}M_x\\ M_\theta\\ M_{x\theta}\end{Bmatrix}=\int_{-\frac{h}{2}}^{\frac{h}{2}}\begin{Bmatrix}\sigma_x\\ \sigma_\theta\\ \tau_{x\theta}\end{Bmatrix}zdz, \tag{11}$$

Eq. (9) will be as

$$U=\int_A\left(N_x\left(\frac{\partial u}{\partial x}+0.5\left(\frac{\partial w}{\partial x}\right)^2\right)-M_x\frac{\partial^2 w}{\partial x^2}+N_\theta\left(\frac{\partial v}{R\partial\theta}+\frac{w}{R}+0.5\left(\frac{\partial w}{R\partial\theta}\right)^2\right)\right.$$
$$\left.-M_\theta\frac{\partial^2 w}{R^2\partial\theta^2}+N_{x\theta}\left(\frac{\partial u}{R\partial\theta}+\frac{\partial v}{\partial x}+\frac{\partial w}{R\partial\theta}\frac{\partial w}{\partial x}\right)-2M_{x\theta}\frac{\partial^2 w}{R\partial\theta\partial x}\right)dA \quad (12)$$

Kinetic energy of the tunnel is as

$$K=\frac{\rho}{2}\int_v\left((\frac{\partial u_1}{\partial t})^2+(\frac{\partial u_2}{\partial t})^2+(\frac{\partial u_3}{\partial t})^2\right)dV, \quad (13)$$

where ρ is the tunnel density. By replacing the movement fields in the above equation, we will have

$$K=\frac{\rho}{2}\int_{-\frac{h}{2}}^{\frac{h}{2}}\int_A\left[(\frac{\partial u}{\partial t})^2-2z\frac{\partial u}{\partial t}\frac{\partial^2 w}{\partial t\partial x}+z^2\left(\frac{\partial^2 u}{\partial t\partial x}\right)^2+(\frac{\partial v}{\partial t})^2-2z\frac{\partial v}{\partial t}\frac{\partial^2 w}{\partial t\partial\theta}\right.$$
$$\left.+z^2\left(\frac{\partial^2 w}{\partial t\partial\theta}\right)^2+(\frac{\partial w}{\partial t})^2\right]dzdA \quad (14)$$

By integration in the thickness direction and considering this fact that the range of integer is symmetric, the odd integers will be zero. So the kinetic energy would be simplified as below:

$$K=\int_A\left(\frac{\rho}{2}\left(\frac{h^3}{12}\left((\frac{\partial^2 u}{\partial t\partial x})^2+(\frac{\partial^2 w}{\partial t\partial\theta})^2\right)\right)+h\left((\frac{\partial u}{\partial t})^2+(\frac{\partial v}{\partial t})^2+(\frac{\partial w}{\partial t})^2\right)\right)dA. \quad (15)$$

External work caused by the blast force is: (Hause and Librescu 2007)

$$W_b=\int(F_{blast})wdA, \quad (16)$$

where Hause and Librescu (2007)

$$F_{blast}=P_{S0}\left[1-\frac{t}{t_0}\right]\exp\left\{\frac{-at}{t_0}\right\}, \quad (17)$$

where P_{S0} is the maximum static pressure and t_0 is positive phase time. That they are:

$$\frac{P_{S0}}{P_0}=\frac{808\left[1+\left(\frac{Z}{4.5}\right)^2\right]}{1+\left(\frac{Z}{0.048}\right)^2\sqrt{1+\left(\frac{Z}{1.35}\right)^2}}, \quad (18)$$

$$\frac{t_0}{W^{1/3}}=\frac{980\left[1+\left(\frac{Z}{0.54}\right)^{10}\right]}{\left[1+\left(\frac{Z}{0.02}\right)^3\right]\left[1+\left(\frac{Z}{0.74}\right)^6\right]\sqrt{1+\left(\frac{Z}{6.9}\right)^2}}, \quad (19)$$

where P_0 is the air pressure.

$$Z=\frac{R}{W^{0.33}}, \quad (20)$$

In the above relation, R is distance from blast centre to surface of structure and W is the explosive mass in terms of Kg. Now, applying Hamilton principle, will lead to the three main equations:

$$\frac{\partial N_x}{\partial x}+\frac{\partial N_{x\theta}}{R\partial\theta}=\rho h\frac{\partial^2 u}{\partial t^2}, \quad (21)$$

$$\frac{\partial N_\theta}{R\partial\theta}+\frac{\partial N_{x\theta}}{\partial x}=\rho h\frac{\partial^2 v}{\partial t^2}, \quad (22)$$

$$\frac{\partial^2 M_x}{\partial x^2}+\frac{2\partial^2 M_{x\theta}}{R\,\partial x\,\partial\theta}+\frac{\partial^2 M_\theta}{R^2\partial\theta^2}-\frac{N_\theta}{R}+N_x\frac{\partial^2 w}{\partial x^2}+N_\theta\frac{\partial^2 w}{R^2\partial\theta^2}$$
$$+N_{x\theta}\frac{2\partial^2 w}{R\partial x\,\partial\theta}+F_{Blast}=\rho h\frac{\partial^2 w}{\partial t^2}, \quad (23)$$

By integrating Eqs. (10) and (11) in the direction of thickness and using Eq. (7), the relationships of the forces and interior moments of the tube can be calculated as

$$N_x=h\left(C_{11}\left(\frac{\partial u}{\partial x}+0.5\left(\frac{\partial w}{\partial x}\right)^2\right)+C_{12}\left(\frac{\partial v}{R\partial\theta}+\frac{w}{R}+0.5\left(\frac{\partial w}{R\partial\theta}\right)^2\right)\right), \quad (24)$$

$$N_\theta=h\left(C_{12}\left(\frac{\partial u}{\partial x}+0.5\left(\frac{\partial w}{\partial x}\right)^2\right)+C_{22}\left(\frac{\partial v}{R\partial\theta}+\frac{w}{R}+0.5\left(\frac{\partial w}{R\partial\theta}\right)^2\right)\right), \quad (25)$$

$$N_{x\theta}=h\left(C_{66}\left(\frac{\partial u}{R\partial\theta}+\frac{\partial v}{\partial x}+\frac{\partial w}{R\partial\theta}\frac{\partial w}{\partial x}\right)\right), \quad (26)$$

$$M_x=\frac{h^3}{12}\left(C_{11}\left(-z\frac{\partial^2 w}{\partial x^2}\right)+C_{12}\left(-z\frac{\partial^2 w}{R^2\partial\theta^2}\right)\right), \quad (27)$$

$$M_\theta=\frac{h^3}{12}\left(C_{12}\left(-z\frac{\partial^2 w}{\partial x^2{}_x}\right)+C_{22}\left(-z\frac{\partial^2 w}{R^2\partial\theta^2}\right)\right), \quad (28)$$

$$M_{x\theta}=\frac{h^3}{12}C_{66}\left(-2z\frac{\partial^2 w}{R\partial\theta\partial x}\right). \quad (29)$$

3. DQM method

DQM is one of the numerical methods in which the governing differential equations are converted to the first order algebraic equations by the weight ratios so that derivative is expressed as a linear sum of weight ratios in a point and the functional amounts there and the other range points in the direction of the coordinate axes. The main relationships of these methods are expressed as the following for a single case (Motezaker *et al.* 2021, Al-Furjan *et al.* 2020, 2021a, b, Kolahchi *et al.* 2015, 2016a, b, 2017):

$$\frac{d^n f_x(x_i,\theta_j)}{dx^n}=\sum_{k=1}^{N_x}A_{ik}^{(n)}f(x_k,\theta_j)\qquad n=1,...,N_x-1. \quad (30)$$

$$\frac{d^m f_y(x_i,\theta_j)}{d\theta^m}=\sum_{l=1}^{N_\theta}B_{jl}^{(m)}f(x_i,\theta_l)\qquad m=1,...,N_\theta-1. \quad (31)$$

$$\frac{d^{n+m}f_{xy}(x_i,\theta_j)}{dx^n d\theta^m}=\sum_{k=1}^{N_x}\sum_{l=1}^{N_\theta}A_{ik}^{(n)}B_{jl}^{(m)}f(x_k,\theta_l). \quad (32)$$

So, it is observed that Selection of the sample points and

weight ratios are two very important and determining factors in the accuracy of DQM method which will be mentioned later. Chebyshev polynomial is widely used for solving the engineering problems and produces good results which is expressed as

$$X_i = \frac{L}{2}\left[1-\cos\left(\frac{i-1}{N_x-1}\right)\pi\right] \qquad i=1,...,N_x \quad (33)$$

$$\theta_i = \frac{2\pi}{2}\left[1-\cos\left(\frac{i-1}{N_\theta-1}\right)\pi\right] \qquad i=1,...,N_\theta \quad (34)$$

The weight ratios are generalized as below for the two dimension case:

a) for the first order derivative:

$$A_{ij}^{(1)} = \begin{cases} \dfrac{M(x_i)}{(x_i-x_j)M(x_j)} & for \quad i\neq j, \quad i,j=1,2,...,N_x \\ -\sum\limits_{\substack{j=1\\ i\neq j}}^{N_x} A_{ij}^{(1)} & for \quad i=j, \quad i,j=1,2,...,N_x \end{cases} \quad (35)$$

$$B_{ij}^{(1)} = \begin{cases} \dfrac{P(\theta_i)}{(\theta_i-\theta_j)P(\theta_j)} & for \quad i\neq j, \quad i,j=1,2,...,N_\theta, \\ -\sum\limits_{\substack{j=1\\ i\neq j}}^{N_\theta} B_{ij}^{(1)} & for \quad i=j, \quad i,j=1,2,...,N_\theta \end{cases} \quad (36)$$

where,

$$M(x_i) = \prod_{\substack{j=1\\ j\neq i}}^{N_x}(x_i-x_j) \quad (37)$$

$$P(\theta_i) = \prod_{\substack{j=1\\ j\neq i}}^{N_\theta}(\theta_i-\theta_j) \quad (38)$$

b) for higher derivative:

$$A_{ij}^{(n)} = n\left(A_{ii}^{(n-1)}A_{ij}^{(1)} - \frac{A_{ij}^{(n-1)}}{(x_i-x_j)}\right) \quad (39)$$

$$B_{ij}^{(m)} = m\left(B_{ii}^{(m-1)}B_{ij}^{(1)} - \frac{B_{ij}^{(m-1)}}{(\theta_i-\theta_j)}\right) \quad (40)$$

So, the final matric form of the motion equations are

$$\left([K]\{d\}+[C]\{\dot{d}\}+[M]\{\ddot{d}\}\right)=\{F\}, \quad (41)$$

In the above relation, there are the stiffness matrix [K], mass matrix [M], damp matrix [C], dynamic amplitude vector of d. Newmark numerical method is used to obtain the time response of the structure under blast load in domain time. According to this method, Eq. (41) is written in the following general form (Kolahchi *et al.* 2021a, b):

$$K^*(d_{i+1}) = Q_{i+1}, \quad (42)$$

where subtitle i + 1 represents time ($t=t_{i+1}$is $K^*(d_{i+1})$) ، effective stiffness matrix and Q_{i+1} is effective load vector written as follows:

$$K^*(d_{i+1}) = K_L + K_{NL}(d_{i+1}) + \alpha_0 M, \quad (43)$$

$$Q_{i+1}^* = F_{i+1} + M\left(\alpha_0 d_i + \alpha_2 \dot{d}_i + \alpha_3 \ddot{d}_i\right), \quad (44)$$

where

$$\alpha_0 = \frac{1}{\chi\Delta t^2}, \quad \alpha_1 = \frac{\gamma}{\chi\Delta t}, \quad \alpha_2 = \frac{1}{\chi\Delta t}, \quad \alpha_3 = \frac{1}{2\chi}-1, \quad \alpha_4 = \frac{\gamma}{\chi}-1, \quad \alpha_5 = \frac{\Delta t}{2}\left(\frac{\gamma}{\chi}-2\right), \quad \alpha_6 = \Delta t(1-\gamma), \quad \alpha_7 = \Delta t\gamma, \quad (45)$$

where γ=0.5 and χ=0.25. Based on repeating method, Eq. (42) is solved at each time amplitude and calculates acceleration and speed modified from the following relations:

$$\ddot{d}_{i+1} = \alpha_0(d_{i+1}-d_i) - \alpha_2\dot{d}_i - \alpha_3\ddot{d}_i, \quad (46)$$

$$\dot{d}_{i+1} = \dot{d}_i + \alpha_6\ddot{d}_i + \alpha_7\ddot{d}_{i+1}, \quad (47)$$

Then, for the next time, we apply acceleration and speed modified into relations (46) and (47) and the steps mentioned are repeated.

4. Results

The numerical results of the blast response in the tunnels considering structural damping is presented in this section based on Hoek-Brown failure criterion and numerical method. The tunnel is made from sandstone with GSI=50, m_b=2.5, s=3.9e-3, a=0.506, density of ρ = 2.5 ge/cm^3 and UCS=80 MPa. The explosive material is ANFO with density of 782 Kg/m^3.

The effect of special weight and GSI of sandstone on the damage factor of tunnel is shown in Figs. 2 and 3. It is found that with increasing the special weight of sandstone, the damage area of the tunnel is reduced. In other words, for sandstone with special weight of 2.3, the damage factor is equal to one in 4.8 m of the thickness while for special weight of 2.7, it is one in 1.45 m of the thickness.

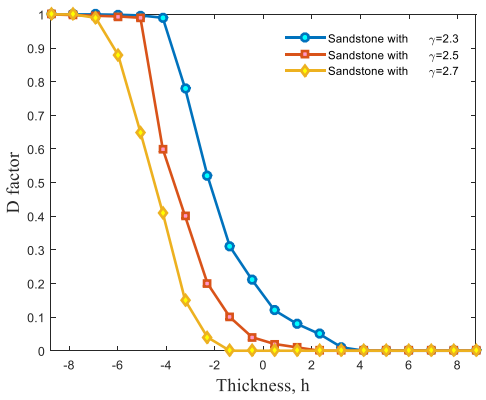

Fig. 2 The effect of special weight of sandstone on the damage factor of tunnel

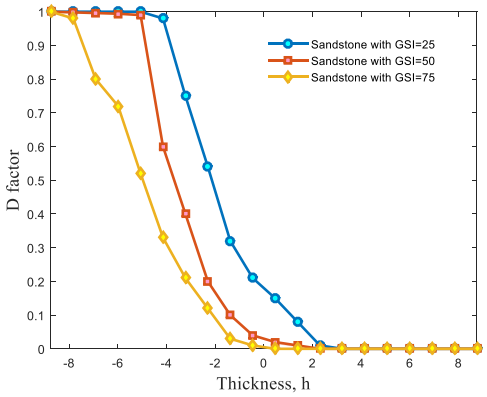

Fig. 3 The effect of special weight of sandstone on the damage factor of tunnel

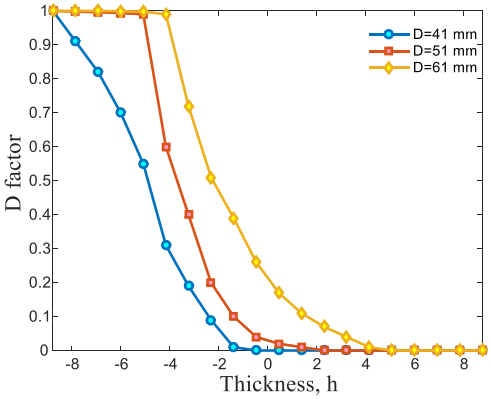

Fig. 6 The effect of blast hole diameter on the damage factor of tunnel

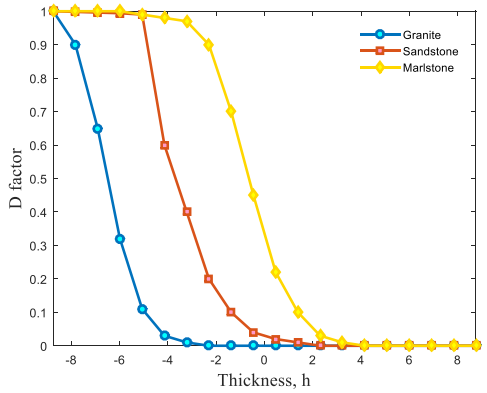

Fig. 4 The effect of tunnel material on the damage factor of tunnel

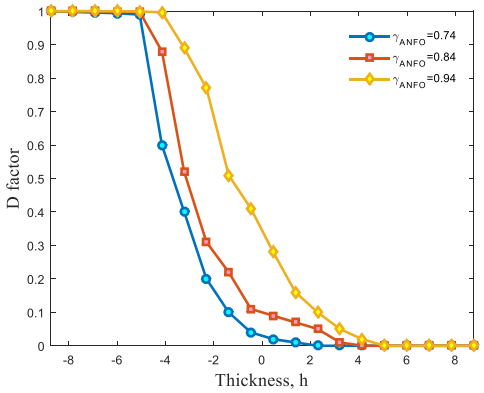

Fig. 7 The effect of special weight of explosive material on the damage factor of tunnel

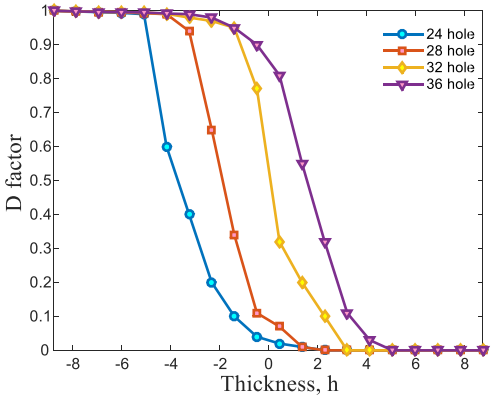

Fig. 5 The effect of blast hole number on the damage factor of tunnel

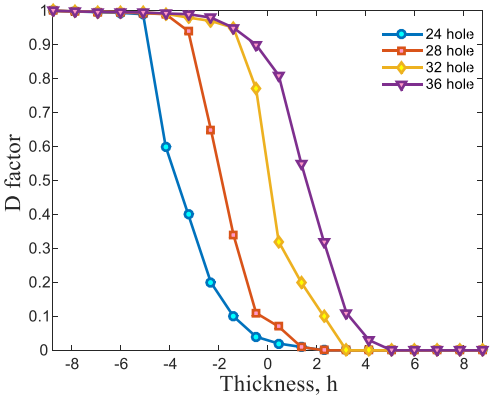

Fig. 8 The effect of mass of explosive material on the damage factor of tunnel

From Fig. 3, it is concluded that with enhancing the GSI of the sandstone, the damage factor of tunnel is decreased significantly. It is due to this fact that with increasing GSI of the sandstone, the stiffness with be enhanced.

The damage factor of the tunnel for sandstone, granite and marlstone is presented in Fig. 4. As can be seen, the damage area for the granite tunnel is lower than sandstone while it is higher for marlstone tunnel. It is since the stiffness of granite is higher than sand stone and marlstone. For example, D is equal to one in 4.2 m of the thickness for sandstone while it is one in only inner surface of tunnel.

The influences of blast hole number, blast hole diameter, special weight and mass of explosive material on the damage factor are illustrated in Figs. 5-8, respectively. From Fig. 5, it is found that with increasing the blast hole number, the damage factor is raised since the dynamic wave induced by blast load is increased.

Fig. 6 shows with enhancing the blast hole diameter, the

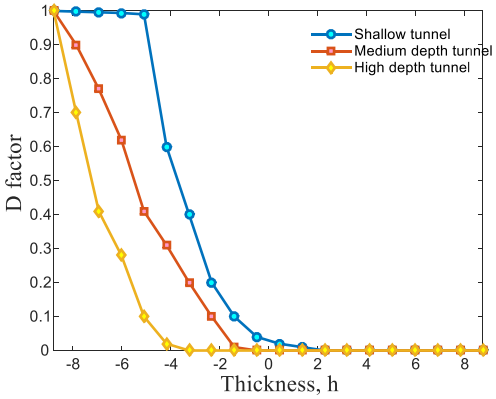

Fig. 9 The effect of tunnel's depth on the damage factor of tunnel

damage factor is increased. It is because with increasing the blast hole diameter, the volume of blast hole is increased and consequently, the explosive materials are enhanced and the induced dynamic wave by clast load will be raised.

From Figs, 7 and 8, it is concluded that with increasing the special weight and mass of explosive material, the damage factor is enhanced. It is physically reasonable, since the dynamic forced of blast load is increased by enhancing the special weight and mass of explosive material.

Fig. 9, demonstrates the effect of tunnel's depth on the damage factor of tunnel. It is observed that with increasing the depth of tunnel, the damage factor is reduced. It is because with increasing the depth of tunnel, the compressive dynamic force applied on the tunnel will be increased.

5. Conclusions

This research analyzed the explosion damage analysis in a tunnel considering structural damping. Different blast holes were assumed in the inner surface of tunnel and the damage factor was calculated by Hoek-Brown failure criterion. The motion equations were derived by cylindrical shell model and Hamilton's principle and solved by numerical mthods of DQ and Newmark. The effect of different parameters such as depth of tunnel, number and diameter of blast holes, type of stone, geological strength index (GSI) and density of stone, type and mass of explosive material were studied on the damage factor of Hoek-Brown criterion. The final results of this research were:

• It was found that with increasing the special weight of sandstone, the damage area of the tunnel was reduced.

• It was concluded that with enhancing the GSI of the sandstone, the damage factor of tunnel was decreased significantly.

• The damage area for the granite tunnel was lower than sandstone while it was higher for marlstone tunnel.

• It was found that with increasing the blast hole number, the damage factor was raised since the dynamic wave induced by blast load was increased.

• With enhancing the blast hole diameter, the damage factor was increased.

• It was concluded that with increasing the special weight and mass of explosive material, the damage factor was enhanced.

• It was observed that with increasing the depth of tunnel, the damage factor was reduced.

References

Al-Furjan, M.S.H., Farrokhian, A., Keshtegar, B., Kolahchi, R. and Trung, N.T. (2020), "Higher order nonlocal viscoelastic strain gradient theory for dynamic buckling analysis of carbon nanocones", *Aerosp. Sci. Technol.*, **107**, 106259. https://doi.org/10.1016/j.ast.2020.106259.

Al-Furjan, M.S.H., Farrokhian, A., Mahmoud, S.R. and Kolahchi, R. (2021a), "Dynamic deflection and contact force histories of graphene platelets reinforced conical shell integrated with magnetostrictive layers subjected to low-velocity impact", *Thin Wall. Struct.*, **163**, 107706. https://doi.org/10.1016/j.tws.2021.107706.

Al-Furjan, M.S.H., Farrokhian, A., Keshtegar, B., Kolahchi, R. and Trung, N.T. (2021b), "Dynamic stability control of viscoelastic nanocomposite piezoelectric sandwich beams resting on Kerr foundation based on exponential piezoelasticity theory", *Eur. J. Mech. A Solid*, **86**, 104169. https://doi.org/10.1016/j.euromechsol.2020.104169.

Chen, Sh.L. and Lee, Sh.Ch. (2020), "An investigation on tunnel deformation behavior of expressway tunnels", *Geomech. Eng.*, **21**(2), 215-226. http://doi.org/10.12989/gae.2020.21.2.215.

Duc, N.D. and Than, P.T. (2015), "Nonlinear dynamic response and vibration of shear deformable imperfect eccentrically stiffened S-FGM circular cylindrical shells surrounded on elastic foundations", *Aerosp. Sci. Technol.*, **40**, 115-127. https://doi.org/10.1016/j.ast.2014.11.005.

Hajihassani, M., Kalatehjari, R., Marto, A., Mohamad, H. and Khosrotash, M. (2020), "3D prediction of tunneling-induced ground movements based on a hybrid ANN and empirical methods", *Eng. Comput.*, **36**, 251-269, https://doi.org/10.1007/s00366-018-00699-5.

Han, Y., Yang, X. and Ni, J. (2020), "Influence of foam liner on tunnels subjected to internal blast loading, green", *Smart Connect. Transport. Syst.*, **20**, 1373-1378. https://doi.org/10.1007/978-981-15-0644-4_103.

Hause, T. and Librescu, L. (2007), "Dynamic response of doubly-curved anisotropic sandwich panels impacted by blast loadings", *Int. J. Solids Struct.*, **44**, 6678-6700. https://doi.org/10.1016/j.ijsolstr.2007.03.006.

Hong, S.K., Oh, D.W., Kong, S.K. and Lee, Y.J. (2020), "Investigation of divergence tunnel excavation according to horizontal offsets between tunnels", *Geomech. Eng.*, **21**(2), 111-122. http://dx.doi.org/10.12989/gae.2020.21.2.111.

Iwano, K., Hashiba, K., Nagae, J. and Fukui, K. (2020), "Reduction of tunnel blasting induced ground vibrations using advanced electronic detonators", *Tunn. Undergr. Sp. Tech.*, **105**, 103556, https://doi.org/10.1016/j.tust.2020.103556.

Katariya, P.V. and Panda, S.K. (2019), "Numerical evaluation of transient deflection and frequency responses of sandwich shell structure using higher order theory and different mechanical loadings", *Eng. Comput.*, **35**, 1009-1026. https://doi.org/10.1007/s00366-018-0646-y.

Keshtegar, B., Farrokhian, A., Kolahchi, R. and Trung, N.T. (2020), "Dynamic stability response of truncated nanocomposite conical shell with magnetostrictive face sheets utilizing higher order theory of sandwich panels", *Eur. J. Mech. A Solid*, **82**, 104010.

https://doi.org/10.1016/j.euromechsol.2020.104010.
Kolahchi. R., Rabani Bidgoli. M., Beygipoor. Gh. and Fakhar, M.H. (2015), A nonlocal nonlinear analysis for buckling in embedded FG-SWCNT-reinforced microplates subjected to magnetic field", *J. Mech. Sci. Tech*., **29**, 3669-3677. https://doi.org/10.1007/s12206-015-0811-9.
Kolahchi, R., Safari, M. and Esmailpour, M. (2016a), "Dynamic stability analysis of temperature-dependent functionally graded CNT-reinforced visco-plates resting on orthotropic elastomeric medium", *Compos. Struct*., **150**, 255-265. https://doi.org/10.1016/j.compstruct.2016.05.023.
Kolahchi, R., Hosseini, H. and Esmailpour, M. (2016b), "Differential cubature and quadrature-Bolotin methods for dynamic stability of embedded piezoelectric nanoplates based on visco-nonlocal-piezoelasticity theories", *Compos. Struct*., **157**, 174-186. https://doi.org/10.1016/j.compstruct.2016.08.032.
Kolahchi, R., Zarei, M.Sh., Hajmohammad, M.H. and Naddaf Oskouei, A. (2017), "Visco-nonlocal-refined Zigzag theories for dynamic buckling of laminated nanoplates using differential cubature-Bolotin methods", *Thin-Wall. Struct*., **113**, 162-169. https://doi.org/10.1016/j.tws.2017.01.016.
Kolahchi, R., Keshtegar, B. and Trung, N.T. (2021a), "Optimization of dynamic properties for laminated multiphase nanocomposite sandwich conical shell in thermal and magnetic conditions", *Int. J. Sandw. Struct*. 10.1177/10996362211020388.
Kolahchi, R. and Kolahdouzan, F. (2021b), "A numerical method for magneto-hygro-thermal dynamic stability analysis of defective quadrilateral graphene sheets using higher order nonlocal strain gradient theory with different movable boundary conditions" *Appl. Math. Model.* **91**, 458-475.
Kumar A., Chakrabartim A. and Bhargavam P. (2013), "Vibration of laminated composites and sandwich shells based on higher order zigzag theory", *Eng. Struct.,* **56**, 880-888.
Li, Y., Yao, W. and Wang, T. (2020), "Free flexural vibration of thin-walled honeycomb sandwich cylindrical shells", *Thin-Wall. Struct*., **157**, 107032. https://doi.org/10.1016/j.engstruct.2013.06.014.
Molkov, V. and Dery, W. (2020), "The blast wave decay correlation for hydrogen tank rupture in a tunnel fire", *Int. J. Hydrogen Energ*., In Press. https://doi.org/10.1016/j.ijhydene.2020.08.062.
Motezaker, M., Kolahchi, R., Rajak, D.K. and Mahmoud, S.R. (2021), "Influences of fiber reinforced polymer layer on the dynamic deflection of concrete pipes containing nanoparticle subjected to earthquake load", *Polym. Composite*, In Press. https://doi.org/10.1002/pc.26118.
Nguyen-Hoang, S. and Phung-Van, P., Natarajan, S. and Kim, H.G. (2016), "A combined scheme of edge-based and node-based smoothed finite element methods for Reissner–Mindlin flat shells", *Eng. Comput*., **32**, 267-284. https://doi.org/10.1007/s00366-015-0416-z.
Rawat, A., Matsagar, V.A. and Nagpal, A.K. (2020), "Free vibration analysis of thin circular cylindrical shell with closure using finite element method", *Int. J. Steel Struct*., **20**, 175-193. https://doi.org/10.1007/s13296-019-00277-5.
Rashiddel, A., Kharghani, M., Dias, D. and Hajihassani, M. (2020), "Numerical study of the segmental tunnel lining behavior under a surface explosion – Impact of the longitudinal joints shape", *Comput. Geotech*., **128**, 103822. https://doi.org/10.1016/j.compgeo.2020.103822.
Reddy, J.N. (2004), *Mechanics of Laminated Composite Plates and Shells*, 2nd Ed., CRC Press, Washington, U.S.A.
Seo, Y.S., Jeong, W.B., Yoo, W.S. and Jeong, H.K. (2015), "Frequency response analysis of cylindrical shells conveying fluid using finite element method", *J. Mech. Sci. Technol*., **19**(2), 625-633. https://doi.org/10.1007/BF02916184.
Skob, Y.A., Ugryumov, M.L. and Granovskiy, E.A. (2021), "Numerical assessment of hydrogen explosion consequences in a mine tunnel", *Int. J. Hydrogen Energ*., **46**(23), 12361-12371. https://doi.org/10.1016/j.ijhydene.2020.09.067.
Tiwari, R., Chakraborty, T. and Matsagar, V. (2020), "Analysis of curved tunnels in soil subjected to internal blast loading", *Acta Geotech*., **15**(2), 509-528. https://doi.org/10.1007/s11440-018-0694-x.
Tran, M.T., Nguyen, V.L., Pham, S.D. and, Rungamornrat, J. (2020), "Free vibration of stiffened functionally graded circular cylindrical shell resting on Winkler–Pasternak foundation with different boundary conditions under thermal environment", *Acta Mech*., **231**(6), 2545-2564. https://doi.org/10.1007/s00707-020-02658-y.
Wu, K., Shao, Zh., Hong, S. and Qin, S. (2020), "Analytical solutions for mechanical response of circular tunnels with double primary linings in squeezing grounds", *Geomech. Eng*., **22**(6), 509-518. http://doi.org/10.12989/gae.2020.22.6.509.
Zaid, M. and Rehan Sadique, Md. (2020), "The response of rock tunnel when subjected to blast loading: Finite element analysis", *Eng. Rep*., **3**(2), e12293. https://doi.org/10.1002/eng2.12293.
Zhang, X., He, Y., Li, Z., Zhai, Zh., Yan, R. and Chen, X. (2020a), "Static and dynamic analysis of cylindrical shell by different kinds of B-spline wavelet finite elements on the interval", *Eng. Comput*., **36**, 1903-1914. https://doi.org/10.1007/s00366-019-00804-2.
Zhang, Sh., Ma, H., Huang, X. and Peng, Sh. (2020b), "Numerical simulation on methane-hydrogen explosion in gas compartment in utility tunnel", *Process Saf. Environ*., **140**, 100-110. https://doi.org/10.1016/j.psep.2020.04.025.
Zhang, X., Zhang, Ch., Min, B. and Xu, Y. (2020), "Experimental study on the mechanical response and failure behavior of double-arch tunnels with cavities behind the liner", *Geomech. Eng*., **20**(5), 399-410. http://doi.org/10.12989/gae.2020.20.5.399.
Zhao, X., Chen, Ch., Shi, C., Chen, J., Chen, Q. and Zhao, D. (2020), "A three-dimensional simulation of the effects of obstacle blockage ratio on the explosion wave in a tunnel", *J. Therm. Anal. Calorim*., **143**, 3245-3256. https://doi.org/10.1007/s10973-020-09777-7.

IC